ACKNOWLEDGMENT

The author is indebted to Dr. Pirini of Telettra S.p.A. (Vimercate, Italy) for kindly making the microstrip lines described in Section V (see Fig. 11).

REFERENCES

[1] Y. Klinger, "The measurement of spurious modes in over-moded waveguides," *Proc. IEE*, vol. 106 B, Suppl. 13, pp. 89–93, 1959.
[2] F. Valdoni, "Misura a risonanza dell'accoppiamento tra modi diversi," *Note Recensioni e Notizie*, vol. XXII, no. 4, pp. 440–449, July 1973.
[3] M. Sucher and J. Fox, *Handbook of Microwave Measurement*, vol. I, 3rd ed. New York: Polytechnic Press, 1963, pp. 359–363.
[4] R. A. Pucel, D. J. Massé, and C. P. Hartwig, "Losses in microstrip," *IEEE Trans. Microwave Theory Techn.*, vol. MTT-16, pp. 342–350, June 1968.
[5] P. Troughton, "Measurement techniques in microstrip," *Electronics Letters*, vol. 5, pp. 25–26, Jan. 23, 1969.
[6] J. H. C. Van Heuven, "Conduction and radiation losses in microstrip," *IEEE Trans. Microwave Theory Techn.*, vol. MTT-22, pp. 841–844, Sept. 1974.
[7] G. C. Corazza and F. Valdoni, "Bipoli Stazionari," *Alta Frequenza*, vol. XLII, pp. 22–26, Jan. 1973.
[8] G. C. Corazza *et al.*, "Multiporte Stazionari," *Alta Frequenza*, vol. XLII, pp. 27–31, Jan. 1973.
[9] V. Rizzoli, "Resonance measurement of even- and odd-mode propagation constants in coupled microstrips," in *IEEE MTT-S International Microwave Symposium Digest* (Palo Alto, CA, May 1975), pp. 106–108.
[10] W. J. Getsinger, "Microstrip dispersion model," *IEEE Trans. Microwave Theory Techn.*, vol. MTT-21, pp. 34–39, Jan. 1973.
[11] J. S. Wight *et al.*, "Equivalent circuits of microstrip impedance discontinuities and launchers," *IEEE Trans. Microwave Theory Techn.* (Short Papers), vol. MTT-22, pp. 48–52, Jan. 1974.
[12] J. Wolff and W. Menzel, "The microstrip double ring resonator," *IEEE Trans. Microwave Theory Techn.*, vol. MTT-23, pp. 441–444, May 1975.
[13] *Advances in Microwaves*, Leo Young, Ed., vol. 8. New York: Academic Press, 1974.
[14] V. Rizzoli, "Losses in microstrip arrays," *Alta Frequenza*, vol. XLIV, pp. 86–94, Feb. 1975.
[15] J. G. Richings and B. Easter, "Measured odd- and even-mode dispersion of coupled microstrip lines," *IEEE Trans. Microwave Theory Techn.*, vol. MTT-23, pp. 826–828, Oct. 1975.
[16] V. Rizzoli, "A unified variational solution to microstrip array problems," *IEEE Trans. Microwave Theory Techn.*, vol. MTT-23, pp. 223–235, Feb. 1975.

A Dual Mode Tuning Circuit for Microwave Transistor Oscillators

ROBERT G. ROGERS, MEMBER, IEEE

Abstract—**A two-port circuit adjusting both even and odd mode fields, with orthogonal mode adjustment, can be used as an embedding circuit for a microwave transistor oscillator. The circuit, analyzed in TEM line, may also be realized in any other form of transmission line geometry, including two coexistent modes in a cavity. The resulting oscillator is stable, has low FM noise, and is readily tunable. Analyses of the tuning circuit and oscillator are presented, along with some experimental results and a discussion of methods using other than TEM transmission lines to produce the even and odd modes.**

I. INTRODUCTION

MICROWAVE transistors vary sufficiently in characteristics between manufacturers and within a type number that an effective oscillator is difficult to obtain satisfying the stringent conditions usually imposed by system requirements.

The transistor embedding circuit described here provides a feedback circuit for a microwave transistor, giving high-quality performance over a good bandwidth. The half-wavelength series element in the tuning circuit serves as the frequency-determining portion of the embedment, and is effectively isolated from the active element, giving frequency stability and low FM noise to the oscillator. The two tuning adjustments of the embedment allow relatively constant power output over a wide tuning range, without further output tuning.

Even and odd mode fields are separately adjusted at the transistor ports to give optimum conditions for oscillation. These fields may be TEM, as presented here, or from higher order modes in stripline, rectangular, cylindrical, or coaxial waveguide.

Manuscript received December 19, 1975; revised July 23, 1976.
The author is with GTE Lenkurt, Inc., San Carlos, CA 94070.

II. THE TUNING NETWORK

Fig. 1 shows the network, considered as air dielectric microstrip above a ground plane. The length l_1 extends from the two ports to the short circuit across conductors; l_2 continues from this short circuit to the grounding of both conductors to the ground plane.

The TEM even and odd mode electric field distributions at the ports are shown in Fig. 2. The short circuit between conductors is odd mode; grounding of both conductors also forms an odd mode short but no odd mode field exists on length l_2. So the odd mode length is l_1 and is adjusted only by changing l_1.

The even mode length is $l_1 + l_2$ but is adjusted only by l_2. With both modes existing at once, it can be seen from Fig. 2 that since the field intensities at the two ports will

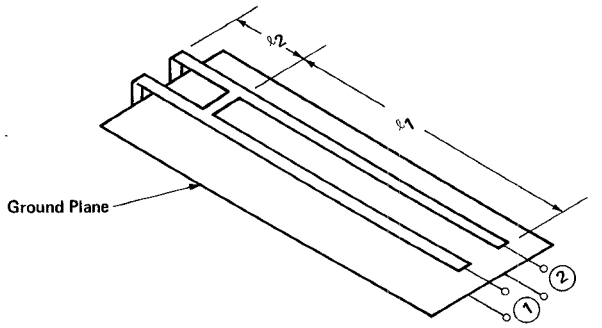

Fig. 1. The double mode circuit in air dielectric microstrip.

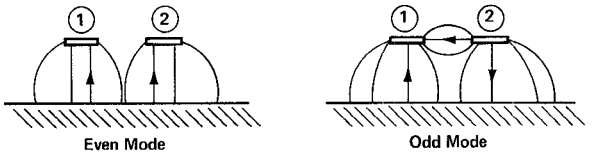

Fig. 2. Even and odd modes at circuit ports.

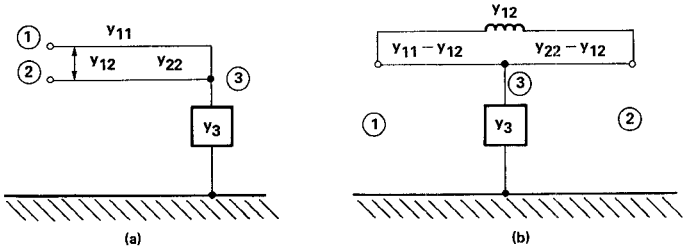

Fig. 3. Coupled transmission line equivalent circuits for analysis.

be the sum of the two modes, their impedance levels can be arbitrarily varied.

The circuit of Fig. 1 can transform any impedance into another arbitrary impedance [1]. This circuit may be analyzed as a coupled transmission line network as shown in Fig. 3(a), where the line of length l_2 is replaced by an admittance y_3 connected to the new port ③. Extracting y_{12} as in Fig. 3(b) leaves the two lines uncoupled [2]. The π network equivalents of the lines, both of length l_1, are shown in Fig. 4. While Fig. 3(b) gives only the characteristic impedances for the elements, Fig. 4 has the complete circuit element quantities; γ is the propagation constant.

Fig. 3 may be used to obtain an admittance matrix which can be manipulated to give the required equivalent circuit of Fig. 5, the original method of solution of the circuit [3]. But the T portion of Fig. 4, internal to the ports, may be converted to a π equivalent and added to the elements across the ports. Then Y_a becomes

$$Y_a = \frac{(y_{11} - y_{12})}{\sinh \gamma l_1} \cdot \left[\frac{(y_{11} + y_{22} - 2y_{12})\left(\coth \gamma l_1 - \frac{1}{\sinh \gamma l_1}\right) + y_3}{(y_{11} + y_{22} - 2y_{12}) \coth \gamma l_1 + y_3}\right] + (y_{11} - y_{12})\left(\coth \gamma l_1 - \frac{1}{\sin \gamma l_1}\right). \quad (1)$$

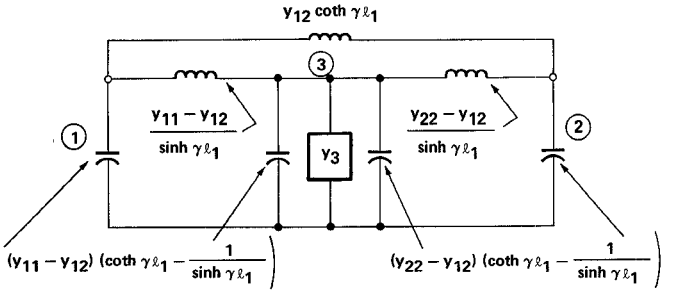

Fig. 4. The complete double mode equivalent circuit of Fig. 3.

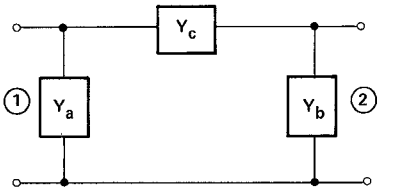

Fig. 5. Equivalent π network of the circuit of Fig. 4.

The first term is that of the shunt arm of the equivalent π of the port ① side of the T (Fig. 4), and the second term is the port ① shunting element.

Manipulation gives

$$Y_a = (y_{11} - y_{12}) \cdot \left[\frac{(y_{11} + y_{22} - 2y_{12}) \sinh \gamma l_1 + y_3 \cosh \gamma l_1}{(y_{11} + y_{22} - 2y_{12}) \cosh \gamma l_1 + y_3 \sinh \gamma l_1}\right] \quad (2)$$

and by interchanging y_{11} and y_{22},

$$Y_b = (y_{22} - y_{12}) \cdot \left[\frac{(y_{11} + y_{22} - 2y_{12}) \sinh \gamma l_1 + y_3 \cosh \gamma l_1}{(y_{11} + y_{22} - 2y_{12}) \cosh \gamma l_1 + y_3 \sinh \gamma l_1}\right]. \quad (3)$$

Then Y_c is

$$Y_c = \frac{(y_{11} - y_{12})(y_{22} - y_{12}) \frac{1}{\sinh \gamma l_1}}{(y_{11} + y_{22} - 2y_{12}) \cosh \gamma l_1 + y_3 \sinh \gamma l_1} + y_{12} \coth \gamma l_1. \quad (4)$$

The y_{ij} are unnormalized admittances of the line [2].

Under the conditions that both conductors are physically identical, which equates y_{11} to y_{22}, the mathematically and practically convenient

$$y_3 = 2(y_{11} - y_{12}) \coth \gamma l_2 \quad (5)$$

is taken. With lossless lines, which equates γ to $j\beta$, (2)–(4) become

$$Y_a = jB_a = jB_b = -jY_{oe} \cot (\beta l_1 + \beta l_2) \quad (6)$$

$$Y_c = jB_c = j\frac{Y_{oe}}{2} \cot (\beta l_1 + \beta l_2) - j\frac{Y_{oo}}{2} \cot \beta l_1. \quad (7)$$

The equivalent circuit is then that of Fig. 6, with decoupled transmission lines, their lengths and characteristic admittances shown, connected by zero electrical length conductors.

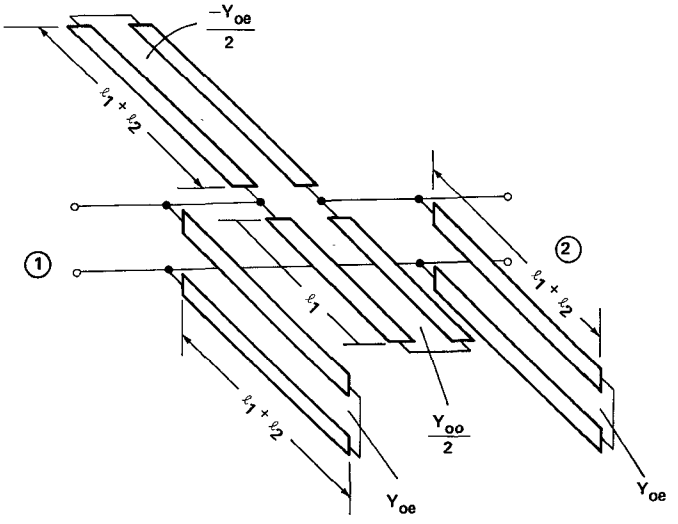

Fig. 6. Equivalent circuit of the network in decoupled transmission lines.

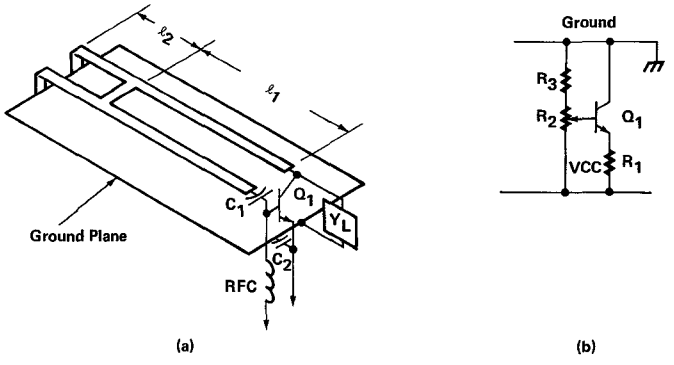

Fig. 7. The circuit of Fig. 1 as an oscillator.

III. Extensions

Any circuit which can produce separately adjustable even and odd mode fields at two ports can be used as an oscillator embedment or impedance matching circuit. In addition to the stripline, microstrip, and coaxial geometries in TEM, cylindrical and rectangular waveguides, waveguide modes in a coaxial line, and higher order modes on stripline may be employed.

For example, coupling to two radial probes in a right circular cylinder, the TE_{11} field gives the odd mode and the TM_{01} field the even mode. Although the TM_{01} has a shorter cutoff wavelength, its resonant frequency may be brought to that of the TE_{11} field by perturbating screws orthogonal to the TE_{11} electric fields.

In a coaxial geometry the TE_{11} field is the odd mode and the TEM the even mode. In rectangular waveguide, two guides coupled through sidewall apertures will produce the required even and odd mode fields.

IV. Oscillator Analysis

Up to now, the circuit of Fig. 1 has been considered only as an impedance matching network. As an oscillator the transistor is connected as shown in Fig. 7(a). The common emitter configuration is used for maximum transistor stability, insuring oscillations at the frequency determined more nearly by the embedding circuit. Due to the requirement of a negative supply, the collector is grounded through the tuning circuit. The base is shunt-fed through the RFC and is coupled to its line by the blocking capacitor C_1.

The emitter is bypassed by C_2, maintaining it at RF ground. The useful load Y_L, yet to be determined, is connected from collector line to ground. Fig. 7(b) shows the bias circuit; R_2 is a potentiometer for varying transistor current. Component values will be given below for specific oscillators.

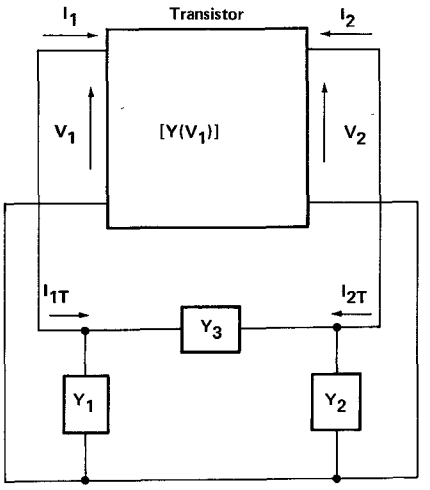

Fig. 8. Oscillator block diagram for analysis.

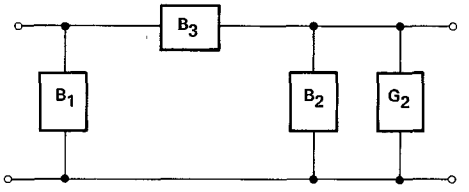

Fig. 9. The required tuning circuit for the oscillator.

Circuit analysis, which follows Vehovec *et al.* [4], uses transistor s parameters of the common emitter connection. The measured s parameters are converted to y parameters to simplify analysis. The circuit is shown in Fig. 8. The six quantities of the embedding network may be reduced to four by setting the real parts of Y_1 and Y_3 to zero. This is a restriction only in that power output resides in the one conductance of Y_2.

The resultant B_1, B_2, and B_3, as derived in the Appendix, are simply required quantities for each frequency, calculated from the transistor y parameters for that frequency. So Fig. 5 must be modified to be that of Fig. 9.

Immediately, B_a may be equated to B_1, and B_c to B_3, but since B_b has also been made equal to B_a, an additional susceptance B_L (Fig. 10) must be added, where

$$B_L = B_2 - B_1. \tag{8}$$

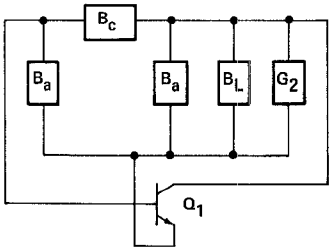

Fig. 10. The double mode tuned oscillator showing transistor and load admittance G_2 and B_L.

So

$$B_1 = -Y_{oe} \cot \beta(l_1 + l_2)$$
$$B_2 = B_L - Y_{oe} \cot \beta(l_1 + l_2)$$
$$B_3 = \frac{Y_{oe}}{2} \cot \beta(l_1 + l_2) - \frac{Y_{oo}}{2} \cot \beta l_1. \quad (9)$$

Note if B_2 were equated to B_a instead, then $-B_L$ would need to appear in the first equation of (9). From (9)

$$\tan \beta l_1 = \frac{-Y_{oo}}{B_1 + 2B_3} \quad (10)$$

$$\tan \beta l_2 = \frac{B_1 Y_{oo} - (B_1 + 2B_3)Y_{oe}}{Y_{oe}Y_{oo} + B_1(B_1 + 2B_3)}. \quad (11)$$

Equating the numerator of (11) to zero gives the conditions for $l_2 = 0$:

$$\frac{Y_{oo}}{Y_{oe}} = 1 + \frac{2B_3}{B_1} \quad (12)$$

which requires that B_1 and B_3 have the same sign since Y_{oo} is always greater than Y_{oe}, at least in a TEM geometry.

Optimum load conductance G_2 has been shown to be [4]

$$G_2 = g_{22}\left(1 - \frac{4g_{11}g_{22}}{(g_{21} + g_{12})^2 + (b_{21} - b_{21})^2}\right) \quad (13)$$

where the transistor quantities are defined by (23) in the Appendix. [These y_{ij} are not to be confused with those of the transmission line in (1) through (5).]

Equation (13) is the optimum load conductance only under the condition that the output-to-input voltage ratio A, as defined by (21), is at its optimum value [4, eq. (7)].

$$A_{opt} = -(y_{21} + y_{12}^*)/2g_{22}.$$

If the two conductors of Fig. 1 were of different sizes, then B_a and B_b would be unequal due to different characteristic admittances; so (5) would become

$$y_3 = -j(Y_{oe1} + Y_{oe2}) \cot \beta l_2 \quad (14)$$

and (2) and (3) would be

$$B_a = -Y_{oe1} \cot (\beta l_1 + \beta l_2) \quad (15)$$

$$B_b = -Y_{oe2} \cot (\beta l_1 + \beta l_2). \quad (16)$$

Equating (15) and (16) to B_1 and B_2, respectively, gives the condition

$$\frac{Y_{oe1}}{Y_{oe2}} = \frac{B_1}{B_2} \quad (17)$$

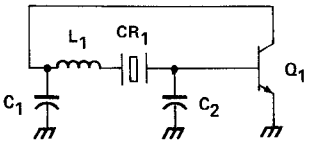

Fig. 11. The Clapp oscillator.

which requires that B_1 and B_2 have the same sign. This eliminates the need for B_L. But now B_c is no longer (7) but

$$B_c = \frac{Y_{oe1}Y_{oe2}}{Y_{oe1} + Y_{oe2}} \cot (\beta l_1 + \beta l_2) + \left[\frac{Y_{oe1}(Y_{oe1} - Y_{oe2})}{Y_{oe1} + Y_{oe2}} - \frac{Y_{oo1}}{2}\right] \cot \beta l_1. \quad (18)$$

The network of Fig. 6 remains unchanged except for the characteristic impedances of the elements.

The cot βl_1 term in (18) may be made zero by use of the physically realizable

$$\frac{Y_{oe2}}{Y_{oe1}} = \frac{2Y_{oe1} - Y_{oo1}}{2Y_{oe1} + Y_{oo1}}. \quad (19)$$

But this reduces (15), (16), and (18) to the all-stop filter section of Matthaei *et al.* [5, fig. 5.09-1(i)].

For the oscillator, (10) and (11) are tuning equations, (8) and (13) give the required load admittance, while (12) indicates whether l_2 may be made zero, and (17) gives the condition for eliminating B_L. The oscillator circuit of Fig. 7(a) has the load admittance $Y_L = G_2 + jB_L$ where the quantities are defined by (13) and (8), respectively.

V. The Practical Oscillator

In the practical oscillator, l_1 is very nearly a half-wavelength in the medium and determines frequency of oscillation almost entirely. Then from the equivalent circuit of Fig. 6 it can be seen that the shunt arms reduce to lines of approximately l_2 in length. And due to the shunting effect of line l_1 in the series arm, the other line, of length $l_1 + l_2$, in the series arm has little effect on series susceptance. Since l_2 in the oscillator is usually nearer a quarter-wavelength, the effect of changing only l_2 is that of tuning the two shunt arms, while changing l_1 tunes the series arm.

That the circuit of Fig. 10 has a high susceptance series arm B_c, does not mean the transistor collector and base are simply shorted together, because the shunt arms hold the complete embedding network attenuation to a finite value just sufficient to match the transistor's gain to give the requirements for oscillation.

This circuit is quite equivalent to the Clapp oscillator [6], [7] still used in high-stability quartz oscillators. Such a circuit, without regard to transistor bias, is shown in Fig. 11. The series arm consists of the quartz crystal CR_1, operating at or near its series resonant mode, and the inductance L_1. The two shunt arms C_1 and C_2, often equal, series resonate with the series arm. Phase shift and attenuation change rapidly with frequency due to the high Q of CR_1. Circuit values are chosen, with C_1 and C_2 relatively large, to give sufficient attenuation to match the transistor's gain.

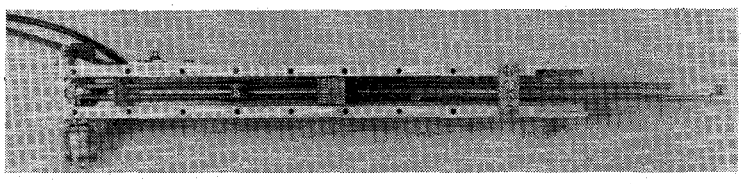

Fig. 12. Double mode coaxial breadboard oscillator.

In the dual mode oscillator circuit of Fig. 10 the shunt arms will not necessarily be capacitive, nor will they resonate with the series arm, as in Fig. 11, because at microwave frequencies the transistor does not cause an 180° phase shift. The series arm of Fig. 10 does not have the Q of a quartz crystal, but still attenuation and phase shift will vary rapidly with frequency.

VI. Oscillator Performance

A final version of the double mode oscillator in a coaxial circuit has been in production for several years. It operates around 2 GHz with a 400-MW output, and has a high-quality linear frequency modulation capability. FM noise is low enough not to need measuring in production. Without need for temperature compensation of the transistor or tuning circuit, frequency drift with temperature over the range of 0–50°C ambient is less than 25 parts per million per degree Celsius; quite adequate for AFC control. Two earlier versions of this product, without frequency modulation capability, are reported.

A. A Coaxial Breadboard Oscillator

Fig. 12 shows the oscillator with cover removed. The coaxial tuning circuit is square in cross section, 0.550 in on a side. The two conductors are of 0.125 in diameter and spaced 0.208 in on centers, centered in the coaxial outer conductor.

Even and odd mode impedances were, respectively, 104 and 38 Ω. They were calculated from static capacitance measurement of two conductors, 6 in long, supported by styrofoam blocks. Measurement was made at 1 mHz. By shorting each line in turn to ground and measuring capacitance between the other line and ground, and by connecting the two lines together and measuring capacitance between them and ground, Z_{oe} and Z_{oo} may be calculated by referring to Mathaei *et al.* [5, fig. 5.05-12 and 5.05-1]. One of the three measurements is redundant for equal conductor size, but serves as a check.

In Fig. 12 the even mode short is about in the center of the picture, with fingers to connect outer conductor walls and the two center conductors. To the left of it is the odd mode short between the two center conductors only. On the left end under the two conductors is the transistor mounted in a bypass and heat-sink assembly. A portion of the bias circuit and supply leads may be seen at the top, a type N output connector is below. The two conductors are held fixed by the clamp at the right, with surplus conductor ends and even mode short circuit drive rod sticking out at the right side.

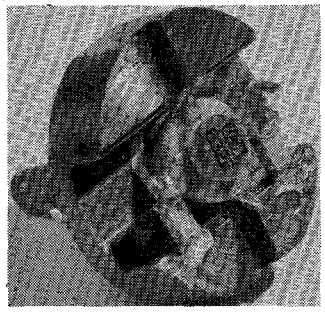

Fig. 13. Transistor mount.

The HP35832E transistor assembly is shown in Fig. 13. The transistor is stud-mounted, designed for stripline, and is of common emitter form. The two emitter leads are bypassed to ground through 100-pF chip capacitors. The collector and base leads are bent up; the former is soldered to the point where the collector and output lines are soldered together. The base lead couples to its line through a 100-pF chip blocking capacitor. Fine wire RFC's to feed-through capacitors supply bias to base and emitter. The bias circuit is that of Fig. 7(b) with the following component values: $R_1 = 23.7\ \Omega$, $R_2 = 500\text{-}\Omega$ potentiometer; $R_3 = 825\ \Omega$.

In addition, a 1.5-μF ceramic capacitor bypasses the base to ground to suppress collector shot noise at baseband frequencies [8], which frequency modulates the oscillator. Collector current shot noise is the largest single source of FM noise in the oscillator.

Fig. 14 shows the tuning characteristics of this oscillator. By means of calipers, l_1 was set to different lengths in 0.200-in increments; then the cover was bolted on and l_2 was adjusted by the drive rod extending out to the right in Fig. 12. Bias supply was -20 V, giving about 18-V collector-to-emitter voltage. Emitter current was held to about 80 mA throughout.

The lowest mode, around 800 mHz, was suppressed to a great extent by a small collector RFC for that purpose. Curve points, particularly l_2, were relatively scattered because of mechanical limitations of the available length of the cavity.

Tuning was smooth, with remarkably constant power output. No output tuning was used; the 50-Ω load is connected directly to the collector tuning line through the type N connector as seen in Fig. 12.

Plotted also are free-space wavelength fractions and l_1

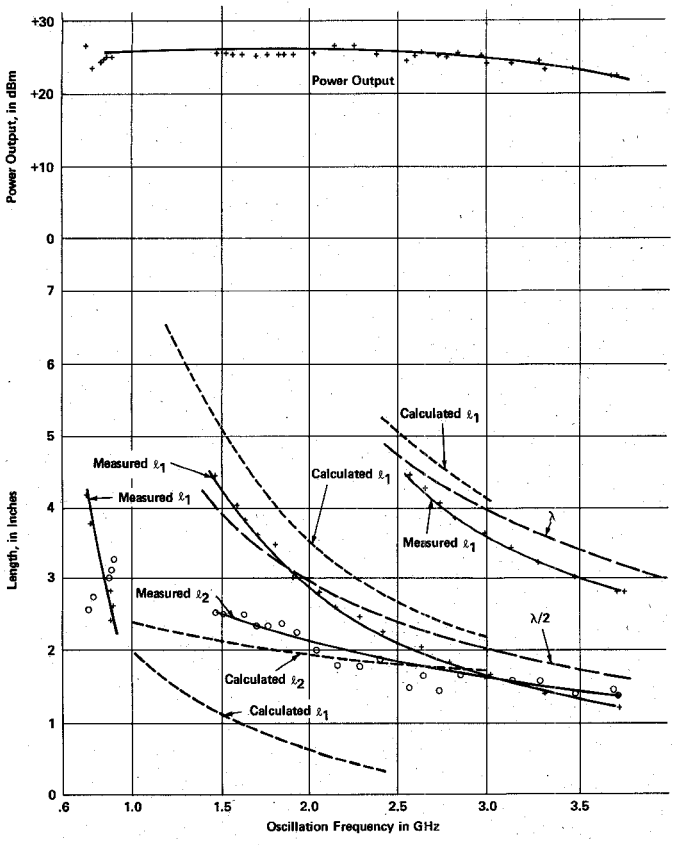

Fig. 14. Tuning and power output of the coaxial breadboard oscillator.

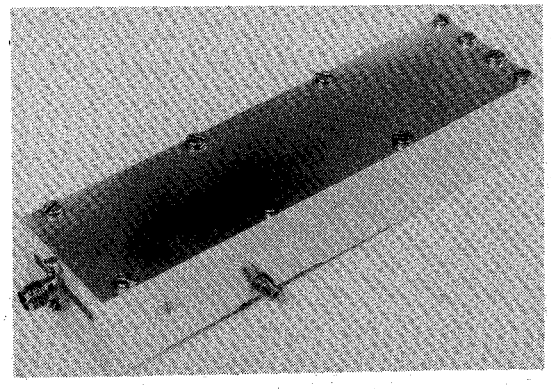

Fig. 15. Stripline oscillator.

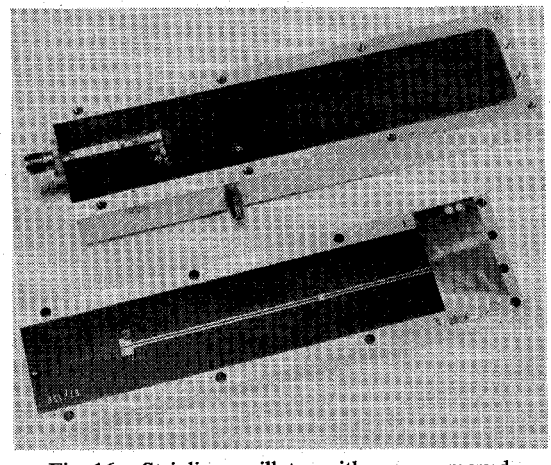

Fig. 16. Stripline oscillator with cover removed.

and l_2 as calculated from (10) and (11), using measured s-parameter values obtained at the operating bias. The two s-parameters S_{11} and S_{21} will decrease as the signal level into the transistors increases toward saturation [9] and by a scalar factor k that is unity with small-signal input and drops to a minimum of 0.5 at high signal level [10]. The calculated curve of Fig. 14 uses k of 0.5. The discrepancy is probably caused by lead lengths of the transistor package.

Power output is also a function of the saturation factor k. While no detailed study is presented, generally at lower frequencies a k of 0.5 gives a better prediction of power output while unity k is better at the transistor's higher frequencies. Indications are that k should be even smaller than 0.5 at higher input levels, but probably not for an oscillator.

Even though oscillation at twice the design frequency can occur, mode jumping is not a problem since l_2 determines the mode: At the second harmonic of the oscillating frequency l_2 is on the order of a half-wavelength, shorting both ports. So no oscillations can occur even though l_1 still yields a high series susceptance at the second harmonic.

Because l_2 is approximately a quarter-wavelength at the frequency of oscillation, second harmonic content in the oscillator output is quite low, difficult to measure. The third harmonic is present but always 30–50 dB down, depending on how close the oscillator has been tuned to the upper performance limits of the transistor.

FM noise was measured under the following conditions:

$l_1 = 3.235$ in
$P_o = 25.2$ dBm
$f = 1.802$ GHz
$l_2 = 2.450$ in
$I_{cc} = 97.4$ mA.

The oscillator signal was converted to 70 mHz by a quiet local oscillator (LO), such as the HP8616A signal generator, and applied to a stock receiver discriminator. The reference level was 200 kHz rms. In a flat 1.75-kHz band centered at the baseband frequency of 70 kHz, the lowest channel normally measured in communications noise tests, and the noisiest, the FM noise was 8.9 Hz rms. Receiver noise power has been subtracted off. If oscillator and LO contribute equally, this is 6.3 Hz rms for the oscillator.

B. Stripline Oscillator

Fig. 15 shows the complete stripline oscillator while Fig. 16 shows the cover removed. The HP35832E transistor is mounted, as in Fig. 13, in a hole in the block below the stripline, the upper part of Fig. 16. Its collector line is soldered to the output strip at the hole through the stripline.

The base lead is soldered to a pad which is coupled to the base tuning circuit pad by means of the visible chip

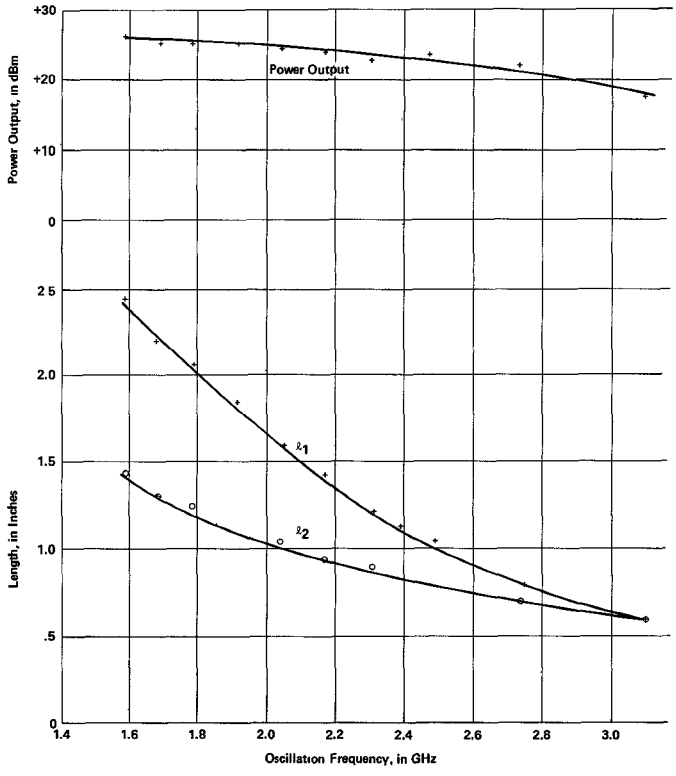

Fig. 17. Tuning and power output of stripline oscillator.

capacitor. The fine wire base RFC extends to a hole in the stripline and by means of a feedthrough capacitor to the bias circuit cavity machined in the other side of the aluminum block.

The cover in the lower portion of Fig. 15 has the two strip conductors which contact the transistor element pads through pads seen at their left end. Copper shim laboratory-type even and odd mode short circuits may be seen to the right. The two conductors are 0.022 in wide separated by 0.015 in. Using [5, eq. (5.05-1-5.05-6)] (Matthaeis *et al.*'s exact thin conductor equations), gave $Z_{oe} = 136\ \Omega$ and $Z_{oo} = 67\ \Omega$. Spacing between stripline ground planes is 0.125 in.

The output circuit was 50 Ω shunted by the two no. 32 wire inductors leading from the output strip seen in the top portion of Fig. 16, running to the bottom and top edges of the stripline. In a final version of the oscillator they would be printed on the stripline.

The tuning curve and power output are plotted in Fig. 17. The power drops somewhat more than that of the breadboard coax, but l_2 tuning was more orderly. Since l_2 could not be easily tuned for optimum power output while in operation, two or three points were explored for optimum power output. Then a smooth curve was faired between them and used as a tuning guide to obtain the points of Fig. 17.

So tuning was done by setting l_1 to various values in 0.200-in increments, and setting l_2 according to the roughed-in curve. The oscillator tuned smoothly with no singularities or difficulties, allowing the curve of Fig. 17 to be used for setting to a desired frequency. Power output dropped a little with rising frequency. The bias circuit is again that of Fig. 7(b) with $R_1 = 26.1\ \Omega$, $R_2 = 500\text{-}\Omega$ potentiometer, and $R_3 = 750\ \Omega$. A 1.0-μF ceramic capacitor again bypassed the base to ground.

Pushing figures for these double mode oscillators are a few megahertz per volt at worst. There was no pushing figure specification imposed. The stripline oscillator has a parabolic pushing figure curve, with turn-around point at −19 V. Between −17 and −22 V the pushing figure magnitude never exceeded 200-kHz/V.

In the stripline oscillator a reflection coefficient of 0.1 rotated through all angles pulled the oscillator from its matched load frequency of 1790 mHz + 10 mHz − 5 mHz. However, due to stringent frequency modulation linearity requirements the oscillator was operated into an isolator, so pulling capabilities were not explored.

VII. Conclusions

The double mode tuning circuit allows flexible operation of microwave transistors in a circuit that effectively isolates the frequency-determining element from external influences. Excellent stability, reproducibility of tuning, and low FM noise are thus realized.

The unique impedance matching circuit, which can use a wide range of transmission line elements, is a practical tuning circuit for wide-band operation of oscillators. Its only drawback is that two dimensions must be adjusted, although only one has a major effect on frequency of oscillation. The two dimensions are normally well ordered, and l_2 may be kept fixed for small frequency changes with little power output penalty.

Appendix
Oscillator Analysis

From Fig. 8 the two conditions for oscillation are that I_1 and I_{1T} sum to zero, as do I_2 and I_{2T} [4]. With G_1 and G_3 identically zero, Vehovec *et al.*'s [4, eq. (3)] reduces to the matrix

$$\begin{bmatrix} G_2 \\ B_1 \\ B_2 \\ B_3 \end{bmatrix} \begin{bmatrix} 0 & 0 & 0 & A_I \\ 0 & 1 & 0 & (1 - A_R) \\ A_R & 0 & -A_I & -A_I \\ A_I & 0 & A_R & -(1 - A_R) \end{bmatrix} = \begin{bmatrix} C \\ D \\ E \\ F \end{bmatrix} \tag{20}$$

where the voltage ratio of V_2 to V_1 is defined by

$$A = \frac{V_2}{V_1} = A_R + jA_I \tag{21}$$

and V_1 and V_2 are defined in Fig. 8. Also,

$$\begin{aligned} C &= -g_{11} - \text{Re}\,(Ay_{12}) \\ D &= -b_{11} - \text{Im}\,(Ay_{12}) \\ E &= -g_{21} - \text{Re}\,(Ay_{22}) \\ F &= -b_{21} - \text{Im}\,(Ay_{22}) \end{aligned} \tag{22}$$

where the transistor

$$y_{ij} = g_{ij} + jb_{ij}. \tag{23}$$

Under these conditions, the required tuning network now looks like Fig. 9.

Solving (20) for the desired quantities,

$$B_1 = D - \frac{(1 - A_R)}{A_I} C \tag{24}$$

$$B_2 = -\frac{C}{A_I} + \frac{A_R C + A_I(A_R F - A_I E)}{A_I(A_R^2 + A_I^2)} \tag{25}$$

$$B_3 = \frac{C}{A_I}. \tag{26}$$

References

[1] R. G. Rogers, "Microwave impedance-matching network," United States Patent 3 745 488, July 10, 1973.
[2] R. Sato and E. G. Cristal, "Simplified analysis of coupled transmission lines," *IEEE Trans. Microwave Theory Tech.*, vol. MTT-18, pp. 122–131, Mar. 1970.
[3] H. J. Orchard, private communication.
[4] M. Vehovec, L. Houselander, and R. Spence, "On oscillator design for maximum power," *IEEE Trans. Circuit Theory* (Corresp.), vol. CT-15, pp. 281–283, Sept. 1968.
[5] G. L. Matthaei, L. Young, and E. M. T. Jones, *Microwave Filters, Impedance-matching Networks and Coupling Structures.* New York: McGraw-Hill, 1964.
[6] J. Clapp, "An inductance-capacitance oscillator of unusual frequency stability," *Proc. IRE*, vol. 36, pp. 356–359, Mar. 1948.
[7] J. Clapp, "Frequency-stable L-C oscillators," *Proc. IRE*, vol. 42, pp. 1295–1300, Aug. 1954.
[8] G. Tobey, J. Graeme, and L. Huelsman, Ed., *Operational Amplifiers.* New York: McGraw-Hill, 1971.
[9] L. Houselander, H. Chow, and R. Spence, "Transistor characterization by effective large-signal two-port parameters," *IEEE J. Solid State Circuits*, vol. SC-5, pp. 77-79, Apr. 1970.
[10] J. Kim, L. Gunderson, and J. Singletary, "Analysis of a microwave resonant feedback oscillator," *IEEE Trans. Microwave Theory Tech.*, vol. MTT-19, pp. 331–332, Mar. 1971.

A Large-Signal Theory for Broad-Band Frequency Converters Using Abrupt Junction Varactor Diodes

FARUQ ABDULLAH AND F. MICHAEL CLAYTON

***Abstract*—A multicurrent design theory is developed for square law varactor frequency converters having a pump frequency much greater than the input signal frequency. Efficiency limits are derived for upconverter operation, showing in particular that any broad-band mixer, where all sideband currents around the pump frequency are allowed to flow, must involve a conversion loss of at least 4.4 dB.**

Consideration of circuit interactions and their effect on upconverter responses leads to a design suitable for systems use in the 5.9–6.4 GHz communication band. Experimental studies of a microstrip realization of this mixer show close agreement with theoretical predictions of its behavior, including a conversion loss less than 7.5 dB over an operating range of 1.3 GHz.

I. Introduction

PRESENT DAY microwave trunk radio systems have repeater stations which commonly employ frequency translation of the modulated carrier to and from an intermediate frequency (usually 70 MHz). The upconversion process is often achieved by mixing with an unmodulated microwave carrier, this operation taking place either in a high-level mixer producing sufficient power for radiation directly, or at a lower level, when the mixer will be followed by some form of RF amplification.

Manuscript received May 30, 1975; revised May 25, 1976.

F. Abdullah was with the General Electric Company, Wembley, England. He is now with the City University, London, EC1, England.
F. M. Clayton is with Telecommunications Research Laboratories, Hirst Research Centre, General Electric Company, Wembley, England.

The high-power pump source required in the former arrangement is usually derived from a low-frequency oscillator by a frequency multiplier chain having a dc to RF efficiency of about 5 percent. Consequently, the power loss in the mixer must be minimized by ensuring that currents at unwanted frequencies do not occur in the diode circuit. Clearly, at least three currents must be allowed to flow, and the majority of theoretical studies [1]–[4] considering the operation of this type of mixer have assumed that only these essential frequencies are present. The main engineering implication of such a design is that filters must be provided which present open circuits at the diode for the frequencies of the principal unwanted intermodulation products and yet allow the wanted currents to flow freely. Thus the resulting upconverter is an inherently narrow-band device, and separate designs are required for each channel of an RF multiplexed communication system.

In contrast, the conversion efficiency of the lower power mixer is not of prime importance, and it is desirable to make this aspect of performance subordinate to the requirement of broad-band operation. If possible, one mixer design should cover a whole microwave frequency band without tuning.

Here we consider one of the simplest broad-band frequency converter circuits—a reflection-type current driven mixer (Fig. 1) with the input and output RF propagating